

Intermittencies on tori: A way to characterize them

Christophe Letellier^{a,*}, Dalila Amroun^b, Gilles Martel^b

^a *Groupe d'Analyse TOpologique et de MOdélisation de SYstèmes Dynamiques, France*

^b *Groupe d'Optique et d'Optronique CORIA UMR 6614, Université de Rouen, Av. de l'Université, BP 12, F-76801 Saint-Etienne du Rouvray cedex, France*

Accepted 2 January 2007

Communicated by Professor M.S. El Naschie

Abstract

Since the three types of intermittency have been theoretically described, many experimental observations of such regimes have been reported. Chaotic behaviors occurring after torus breakdowns and quasi-periodic regimes are also very often observed. It is not so surprising that intermittencies on tori were never reported as soon as it is understood that these common characteristic of intermittencies should be investigated in a Poincaré section of a Poincaré section, that is, in a set which is not possible to define. A specific approach is therefore required to identify them as shown in the paper with two examples of type-I intermittency on tori solution to two different systems.

© 2007 Elsevier Ltd. All rights reserved.

1. Introduction

Since the theoretical description of the three types of intermittency by Pomeau and Manneville [1], many observations of intermittent behaviors have been reported in hydrodynamics [2,3], electronics [4,5], and laser dynamics [6–9]. Intermittent behaviors are very important since they are among the most important routes to chaos with the period-doubling cascade and the Newhouse–Ruelle–Takens scenario [10]. In the latter scenario, few successive Hopf bifurcations imply a quasi-periodic regime and then a chaotic behavior. Quasi-periodic regimes are characterized by phase portraits structured on tori. From quasi-periodic regimes, many routes to chaos can be distinguished [11,12]. The most common route is a torus breakdown as described by the Curry–Yorke scenario [13]. More rarely observed is the torus breakdown through a crisis with an unstable periodic orbits [14] which is associated with a type-II intermittency [15]. Such a scenario has been observed in a glow discharge plasma [16].

Another route to chaos from a quasi-periodic regime is the period-doubling cascade on tori [17–20]. In such a case, Poincaré sections look like period-1, period-2, period-4 limit cycles and so on up to a Rössler-like chaotic attractor. The main difference with the usual Rössler system is that the Rössler-like structure in the Poincaré section is obtained from many points in the Poincaré section, the full picture arising point after point, and not from a simple continuous trajectory. The key point is that the unimodal map with a differentiable maximum necessarily associated with any period-

* Corresponding author. Tel.: +33 2 35 146557; fax: +33 2 35 708384.
E-mail address: Christophe.Letellier@coria.fr (C. Letellier).

doubling cascade cannot be drawn since it would require to compute a Poincaré section of a Poincaré section, a set which cannot be defined.

The subsequent part of this paper is organized as follows. Section 2 is devoted to a simple case of type-I intermittency solution to a detuned monomode laser system. Section 3 discusses a more complicated case where there is no possibility to identify a variable allowing to reach the usual characteristics. Section 4 gives the conclusion.

2. A simple example in a detuned laser

As for any system associated with a unimodal map with a differentiable maximum, a type-I intermittency must be identified before each “periodic-window”, as observed in a bifurcation diagram of the logistic map. For a system with a period-doubling cascade on tori, a “periodic-window” corresponds to a quasi-periodic regime structured on a T^2 torus. The two frequencies are (i) the frequency f_1 around the rotation axis and (ii) the frequency f_2 with which the trajectory turns along the section of the torus. In a “periodic-window”, a sub-harmonic of the main frequency occurs and the torus can no longer be embedded in a 3D space since its Poincaré section thus has self-intersections. The corresponding quasi-periodic regime is therefore embedded in a space with a dimension at least equal to 4.

A very first example of type-I intermittency on tori is observed in a detuned monomode laser, described by the Zeghlache–Mandel system [22]

$$\begin{cases} \dot{x}_1 = -\sigma x_1 + \sigma y_1 \\ \dot{x}_2 = -\sigma x_2 + \sigma y_2 \\ \dot{y}_1 = -y_1 - \delta y_2 + x_1 z \\ \dot{y}_2 = -y_2 + \delta y_1 + x_2 z \\ \dot{z} = -\gamma(z - R + x_1 y_1 + x_2 y_2) \end{cases} \quad (1)$$

where $x_1 = \Re(e)$ and $x_2 = \Im(e)$ are the normalized electric field amplitudes, $y_1 = \Re(p)$ and $y_2 = \Im(p)$ the normalized polarizations and $z = d$ the normalized population inversion. R is the pumping rate, σ is the ratio of the cavity decay rate of the field over the decay rate of the polarisation and γ is the normalized relaxation rate of the inversion. These equations are invariant under the symmetry $U(1) : (e, p, d) \rightarrow (e e^{i\theta}, p e^{i\theta}, d)$, that is, a continuous rotation symmetry [20]. The detuning δ of the field frequency from the atomic resonance transition frequency induces the continuous rotation symmetry. When $\delta = 0$ and with a coordinate transformation, the system reduces to the Lorenz system. Any behavior observed on the Lorenz system can therefore be observed in the Zeghlache–Mandel system, but conjugated with a rotation symmetry ($\delta \neq 0$). A limit cycle of the Lorenz system thus becomes a quasi-periodic regime for the Zeghlache–Mandel system.

The time evolution of the z -variable is characteristic of the type-I intermittency alternating laminar phases and chaotic bursts (Fig. 1a). In the z -induced differential embedding, that is, a space spanned by the z -variable and its successive time derivatives, the laminar phases are associated with the trajectory close to the ghost period-3 limit cycle. Using the intensity $I = x_1^2 + x_2^2$ – the common physical quantity recorded in laser experiments – provides similar results as for the z -variable since, in this example, it modds out the phase θ due to the detuning δ .

The z -variable of system (1) is invariant under the symmetry and any dynamical regime can be easily identified using the differential embedding induced by this variable [20]. For instance, the tangent bifurcation associated with the type-I intermittency before the “period-3 window” can be evidenced using a third-return map to a Poincaré section (Fig. 2).

Modding out the phase is not always sufficient to recover the underlying Lorenz dynamics. There are some laser systems for which the spatial effect blurs the structure when seen from the inversion as well as from the intensity

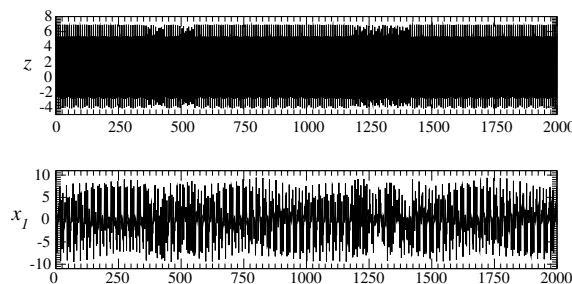


Fig. 1. Time series of the z - and x_I -variables of system (1) for $R = 22$, $\delta = 0.66077$, $\gamma = 0.5$ and $\sigma = 2$.

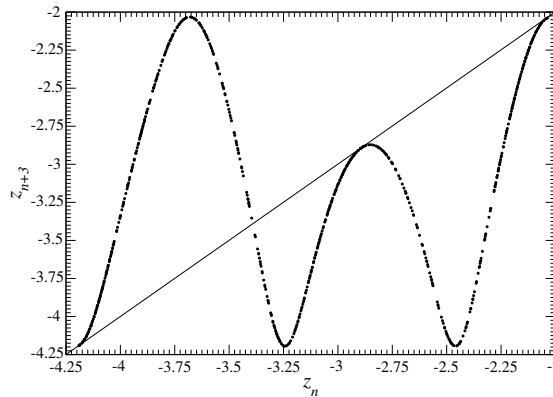


Fig. 2. Third-return map to a Poincaré section of the differential embedding induced by the z -variables of the Zeghlache–Mandel system for $R = 22$, $\delta = 0.66077$, $\gamma = 0.5$ and $\sigma = 2$. Three tangencies between the map and the bisecting line clearly identify the type-I intermittency.

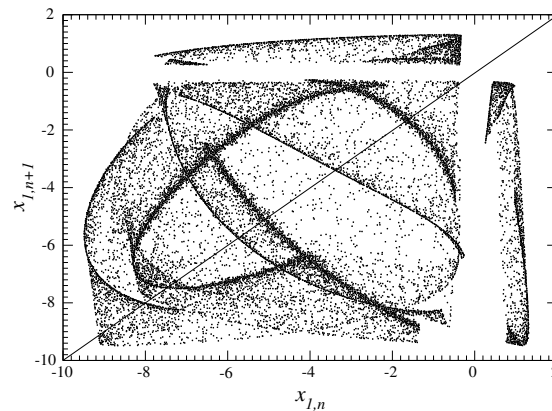


Fig. 3. First-return map to a Poincaré section (50,000 points) of the differential embedding induced by the variable x_1 of system (1) for $R = 22$, $\delta = 0.66077$, $\gamma = 0.5$ and $\sigma = 2$.

[21]. Since in the present case, the type-I intermittency is well identified, it is interesting to investigate how it is possible to exhibit the type of intermittency when it is impossible to compute a map with the expected tangencies.

Indeed, when the x_1 -variable of system (1) is recorded, it is difficult to identify an intermittency (Fig. 1b). The third-return map (not shown) to the Poincaré section defined by $\dot{x}_1 = 0$ and $\ddot{x}_1 > 0$ does not present the three tangencies as shown in Fig. 2.

Using a first-return map helps to obtain a simpler structure (Fig. 3). This map clearly presents a mostly visited structure which, by definition, corresponds to the laminar phases. It can therefore be used to distinguish laminar phases from chaotic bursts. This is done by using a grid (400×400) and counting how many times the trajectory visits the pixels. A pixel P_{ij} is associated with laminar phases when it is visited more than a given number of times. The structure associated with laminar phases is thus identified (Fig. 4a) as well as chaotic bursts (Fig. 4b). It is then straightforward to compute the distribution $D(N)$ of laminar lengths N . In the present case, the distribution (Fig. 5) reveals that there are one short and one long preferred lengths as expected for a type-I intermittency. We therefore have characterized this intermittency.

3. A more complicated example in a bimode laser

Let us now investigate an example of type-I intermittency on tori observed in a system which does not have a variable allowing an easy identification of the intermittent behavior. This is the case for the four dimensional autonomous bimode laser model [23,24]

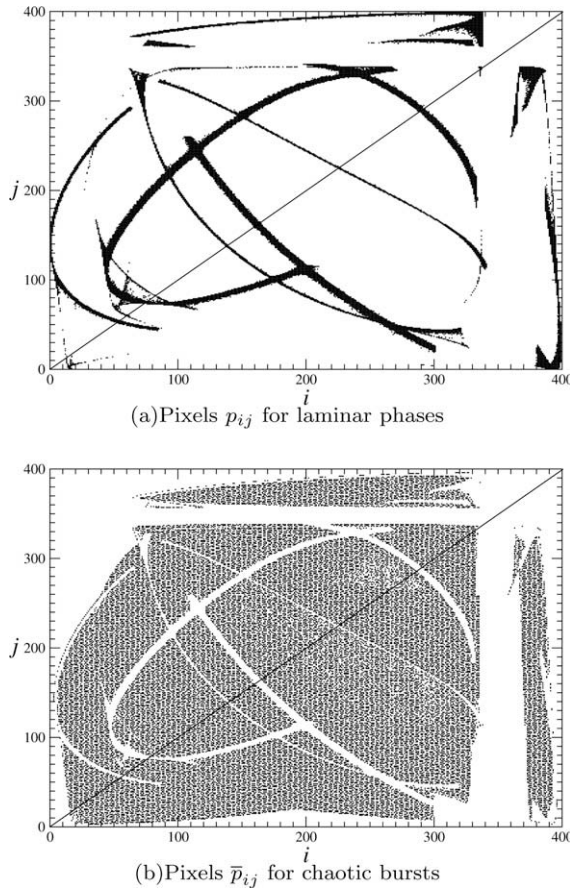


Fig. 4. Structure associated with laminar phases (a) and chaotic bursts (b). Pixels p_{ij} associated with laminar phases are selected in saving pixels visited more than 40 times over $5 \cdot 10^6$ points. Same parameter values as for Fig. 3. (a) Pixels p_{ij} for laminar phases. (b) Pixels \bar{p}_{ij} for chaotic bursts.

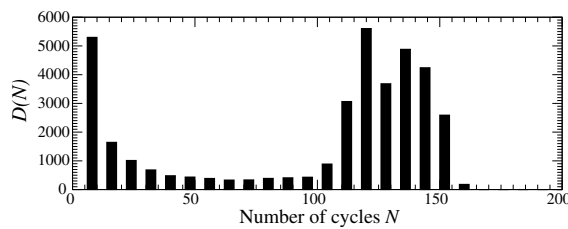


Fig. 5. Distribution of laminar lengths for the system (1) with $R = 22$, $\delta = 0.66077$, $\gamma = 0.5$ and $\sigma = 2$.

$$\begin{cases} \dot{x}_1 = A - x_1 - (y_1 + \beta y_2)x_1 \\ \dot{x}_2 = \gamma A - x_2 - (y_2 + \beta y_1)x_2 \\ \dot{y}_1 = \kappa \left(-1 + (x_1 + \beta x_2) - \frac{\alpha}{1 + \alpha(y_1 + y_2)} \right) y_1 \\ \dot{y}_2 = \kappa \left(-1 + (x_2 + \beta x_1) - \frac{\alpha}{1 + \alpha(y_1 + y_2)} \right) y_2 \end{cases} \quad (2)$$

Each polarized mode is described by its normalized intensity (y_1 or y_2) and its normalized population inversion (x_1 or x_2) [23]. The initial conditions are $x_1 = \frac{A}{1 + u_1 + \beta u_2}$, $x_2 = \frac{\gamma A}{1 + u_2 + \beta u_1}$, $y_1 = 0.01u_1$ and $y_2 = 0.01u_2$ where $u_1 = 0.445013$ and

$u_2 = 0.010008$. With $\beta = 0.5$, $\kappa = 5000$, $\alpha = 0.005$, $\gamma = 0.85$, $a = 0.8$ and $\Lambda = 2.889$, there is a torus with three loops (Fig. 6) on which a period-doubling cascade occurs.

This torus results from the incommensurate frequencies associated with the two modes. There is no symmetry properties involved here. Increasing the pumping rate Λ , a period-doubling cascade on tori is observed and, then, chaotic

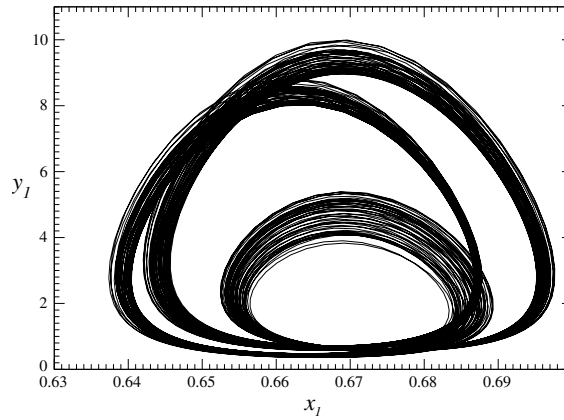


Fig. 6. A quasi-periodic regime solution to model (2) with $\Lambda = 2.889$. Other parameter values are $\beta = 0.5$, $\kappa = 5000$, $\alpha = 0.005$, $\gamma = 0.85$ and $a = 0.8$.

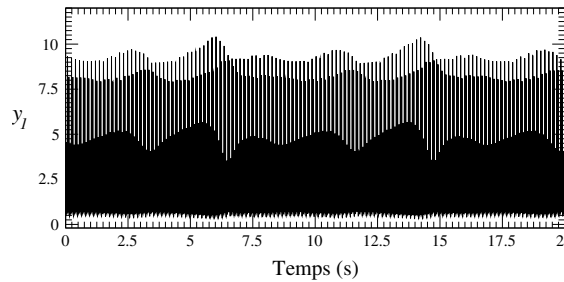


Fig. 7. Time series of intensity y_1 of the bimode laser for the type-I intermittency. Parameter values: $\beta = 0.5$, $\kappa = 5000$, $\alpha = 0.005$, $\gamma = 0.85$, $a = 0.8$, $\Lambda = 2.902666$.

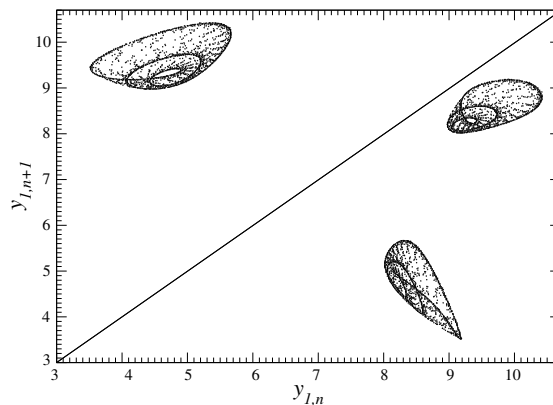


Fig. 8. First-return map to a Poincaré section for model (2). Same parameter values as in Fig. 7.

regimes with periodic windows. For $A = 2.9027$, a quasi-periodic regime associated with the period-3 window is observed. a type-I intermittency is observed but there is no variable of system (2) which presents obvious characteristics of an intermittent behavior (Fig. 7).

The “period-3 orbit” is evidenced by the mostly visited structure in the first-return map to the Poincaré section defined by $\dot{x}_1 = 0$ and $\ddot{x}_1 > 0$ (Fig. 8). Using the procedure previously described, laminar phases (Fig. 9a) are distinguished from chaotic bursts (Fig. 9b) and the distribution of laminar lengths is computed. The typical distribution (one peak for short lengths and one peak for long lengths) is recovered as expected (see Fig. 10). Thus, although it is not possible to identify the tangent bifurcation always associated with a type-I intermittency, some of its characteristics are still identified.

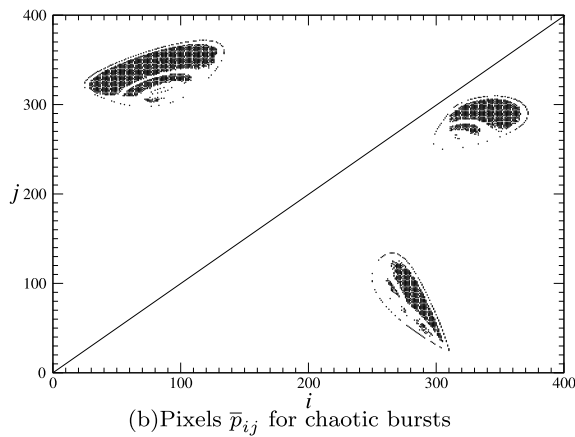
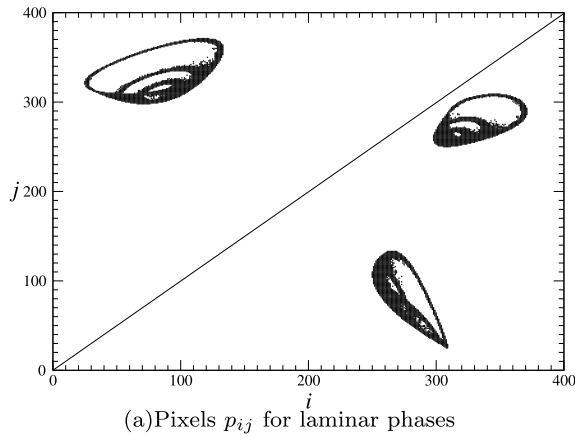


Fig. 9. Structure associated with the laminar phases (a) and the chaotic bursts (b). Same parameter values as for Fig. 7. (a) Pixels p_{ij} for laminar phases. (b) Pixels \bar{p}_{ij} for chaotic bursts.

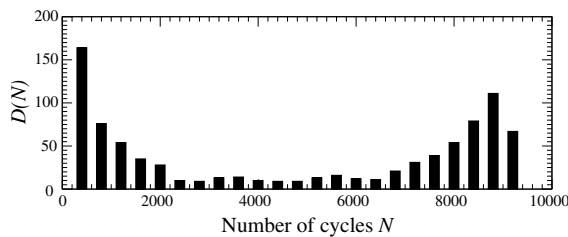


Fig. 10. Distribution of laminar lengths. Same parameter values as for Fig. 7.

4. Conclusion

Using two different laser systems, two examples of intermittencies on tori have been investigated. Although the tangent bifurcation cannot be identified, we showed that return maps to a Poincaré section can still be used to identify the type of intermittent behaviors on tori. These results should help to focus attention to intermittencies on tori which are very few (or never) reported in the literature.

Acknowledgement

We thank Robert Gilmore for fruitful discussions and encouragements.

References

- [1] Pomeau Y, Manneville P. *Comm Math Phys* 1980;74:189–97.
- [2] Bergé P, Dubois M, Manneville P, Pomeau Y. *J Phys (Lett)* 1980;41:L344.
- [3] Ringuet E, Rozé C, Gouesbet G. *Phys Rev E* 1993;47(2):1405–7.
- [4] Jeffries C, Perez J. *Phys Rev A* 1982;26(4):2117–22.
- [5] Huang J-Y, Kim J-J. *Phys Rev A* 1987;36(3):1495–7.
- [6] Sacher J, Elsässer W, Göbel EO. *Phys Rev Lett* 1989;63(20):2224–7.
- [7] Tang DY, Pujol J, Weiss CO. *Phys Rev A* 1991;44(1):R35–8.
- [8] Pujol J, Arjona M, Corbalán R. *Phys Rev A* 1993;48(3):2251–5.
- [9] San-Martin J, Antoranz JC. *Phys Lett A* 1996;219:69–73.
- [10] Newhouse S, Ruelle D, Takens F. *Comm Math Phys* 1978;64:35.
- [11] Aroson DG, Chory MA, Hall GR, McGhee RP. *Comm Math Phys* 1982;83:303.
- [12] Ostlund S, Rand D, Sethna J, Siggia E. *Physica D* 1983;8:303.
- [13] Curry J, Yorke JA. *Lect Notes Math* 1977;668:48.
- [14] Baptista MS, Caldas IL. *Phys Rev E* 1998;58(4):4413–20.
- [15] Baptista MS, Caldas IL. *Physica D* 1999;132:325–38.
- [16] Letellier C, Dinklage A, El-Naggar H, Wilke C, Bonhomme G. *Phys Rev E* 2001;63:042702.
- [17] Arnéodo A, Coulet PH, Spiegel EA. *Phys Lett A* 1983;94(1):1.
- [18] Basset MR, Hudson JL. *Physica D* 1989;35:289–98.
- [19] Flesseles J-M, Croquette V, Jucquois S. *Phys Rev Lett* 1994;72(18):2871–4.
- [20] Letellier C. *Int J Bif Chaos* 2003;13(6):2871–4.
- [21] Amroun D, Brunel M, Letellier C, Leblond H, Sanchez F. *Physica D* 2005;203(3–4):185–97.
- [22] Zeghlache H, Mandel P. *J Opt Soc Am B* 1985;2:18–22.
- [23] Martel G, Bennoud M, Ortac B, Chartier T, Nunzi J-M, Boudebs G, et al. *J Mod Opt* 2004;51(1):85–95.
- [24] Letellier C, Bennoud M, Martel G. *Chaos, Solitons & Fractals* 2007;33(3):782–94.